Supporting Information (SI)

Extraordinary Electrochemical Stability and Extended Polaron Delocalization of Ladder-Type Polyaniline-Analogous Polymers

Xiaozhou Ji,[1] Mingwan Leng,[1] Haomiao Xie,[1] Chenxu Wang,[2] Kim R. Dunbar,[1] Yang Zou,[3]* and Lei Fang[1,2]*

[1] Department of Chemistry, Texas A&M University, College Station, TX 77843-3255, USA

[2] Department of Materials Science and Engineering, Texas A&M University, College Station, TX 77843-3255, USA

[3]Shenzhen Key Laboratory of Polymer Science and Technology, College of Materials Science and Engineering, Shenzhen University, Shenzhen 518060, China

***Correspondence Address**

Professor Yang Zou
Shenzhen Key Laboratory of Polymer Science and Technology
College of Materials Science and Engineering, Shenzhen University,
Shenzhen, 518060, China
Tel: +86-13632949500
E-Mail: yangzou@szu.edu.cn

Professor Lei Fang
Department of Chemistry, Texas A&M University, 3255 TAMU
College Station, TX 77843-3255, USA
Tel: +1 (979) 845 3186
E-Mail: fang@chem.tamu.edu

TABLE OF CONTENTS

1. General Method

All reaction solvents were dried and purified by an Inert Technology pure solvent system (PureSolv-MD-5a). All starting materials were obtained from commercial suppliers and were used without further purification unless otherwise specified. ^{1}H, ^{13}C, ^{1}H-^{13}C HSQC and ^{1}H-^{13}C HMBC nuclear magnetic resonance (NMR) spectra were recorded on a Varian Inova 500 MHz spectrometer at room temperature and processed by MestReNova. Chemical shifts are reported in ppm relative to the signals corresponding to the residual non-deuterated solvents (for ^{1}H NMR: d8-THF δ = 3.58 ppm; for ^{13}C NMR: d8-THF δ = 67.21 ppm). Flash column chromatography purifications were carried out using a Biotage® Isolera™ Prime with various sizes of SiO_2 Biotage SNAP® cartridges. Size Exclusive Chromatography (SEC) was performed on a TOSOH EcoSEC (HLC-8320GPC) chromatography at 40 ºC with UV detector at 254 nm and THF as the eluent. The molecular weights were calculated using a calibration curve based on the UV absorption signal of polystyrene standards. UV-Vis-NIR absorption spectra were recorded on a Hitachi U-4100 UV-Vis-NIR spectrophotometer. Electrospray ionization mass spectrometry (ESI-MS) experiments were performed using a Thermo Scientific Q-Exactive Focus operated in full MS in positive mode. FT-IR spectra were recorded in attenuated total reflectance mode (with ZnSe) using a Shimadzu IRAffinity-1S spectrometer. Cyclic Voltammetry (CV) and controlled potential experiments were performed with a Gamry Interface 1010 T potentiostat. Electron paramagnetic resonance (EPR) spectroscopy was conducted on a Bruker ELEXSYS II E500 with microwave frequency of ca. 9.38 GHz at 288 K. Elemental analysis was performed by Robertson Microlit Laboratories.

2. Synthesis

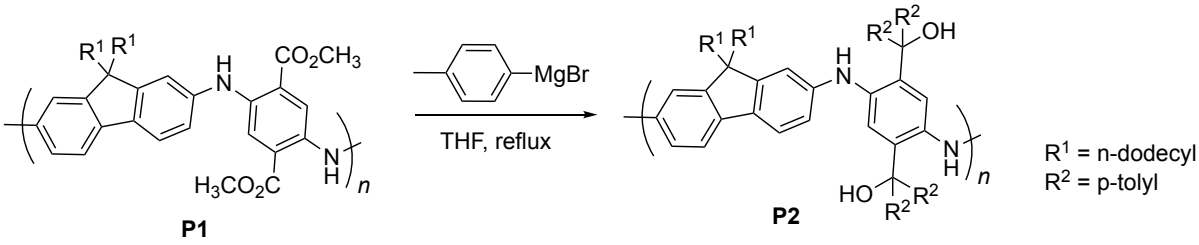

P2: **P1** ($M_{n,\,SEC}$ = 25.9 kg/mol, $Đ$ = 2.23) was synthesized according to a previously reported procedure.[1] To a solution of *p*-tolyl magnesium bromide in tetrahydrofuran (THF) (1.5 mL, 1.0 M) under N_2 protection, **P1** solution (0.10 g) in THF (5 mL) was added dropwise. The reaction was heated to reflux for 12 h. After cooled to room temperature, the mixture was poured into saturated NH_4Cl aqueous solution. The solid precipitate was filtered and dried under vacuum, affording a dark blue solid as **P2** (0.13 g, 91%). ^{1}H NMR (500 MHz, THF-*d*8, 298 K) δ 7.25 – 6.86 (m, 16H), 6.67 (s, 2H), 6.40 (s, 4H), 6.23 (s, 2H), 2.90 (br, 2H), 2.19 (s, 12H), 1.70 (m, 4H), 1.35 – 0.94 (m, 36H), 0.87 (t, J = 6.9 Hz, 6H), 0.56 (m, 4H). ^{13}C NMR (126 MHz, THF-*d*8, 298 K) δ 151.44, 144.80, 143.45, 137.98, 136.54, 134.32, 128.77, 128.20, 125.70, 123.60, 118.65, 115.90, 112.14, 82.70, 67.56, 67.39, 67.21, 67.03, 66.86, 54.87, 41.19, 34.91, 32.69, 31.27, 30.80, 30.49, 30.45, 30.13, 25.45, 25.29, 25.14, 24.98, 24.82, 23.38, 21.07, 14.29. FT-IR (ATR) (cm^{-1}): 3544, 3379, 3028, 2923, 2854, 1608, 1504, 1460, 1392, 1264, 1020, 812. Size exclusion chromatography: M_n = 20.7 kg/mol, $Đ$ = 2.54. The decreased of measured M_n of **P2** was attributed to the removal of higher molecular weight fraction during the work-up process.

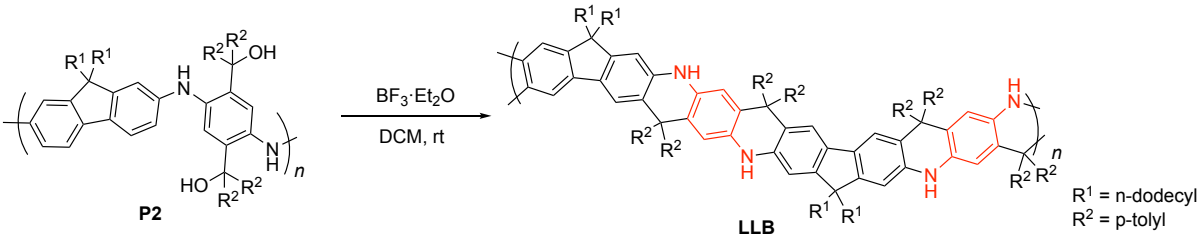

LLB: In a **P2** (0.13 g) solution in CH_2Cl_2 (10 mL), $BF_3{\cdot}Et_2O$ (0.25 mL, 0.3 M) was added and the mixture was stirred at room temperature under N_2 protection for 12 h. The reaction was

quenched by adding into aqueous NaOH solution (1 M). The resulting precipitate was filtered, washed with acetone, and dried under vacuum, affording a brown solid as **LLB** (0.10 g, 84%). ^{1}H NMR (500 MHz, THF-*d*8, 298 K) δ 7.77 (br, 4H), 6.86 (dd, J = 58.2, 7.7 Hz, 32H), 6.62 (s, 4H), 6.51 (s, 4H), 6.37 (s, 4H), 2.29 (s, 24H), 1.35 – 0.95 (m, 80H), 0.86 (m, 20H). ^{13}C NMR (126 MHz, THF-*d*8, 298 K) δ 150.50, 150.20, 144.95, 142.78, 142.18, 135.78, 134.86, 133.03, 131.04, 128.70, 127.96, 126.98, 126.60, 125.61, 122.93, 121.76, 118.87, 115.42, 107.96, 57.18, 55.03, 41.45, 32.66, 30.93, 30.40, 30.17, 30.09, 23.37, 20.89, 14.28. FT-IR (ATR) (cm^{-1}): 3423, 3385, 2922, 2949, 1617, 1492, 1455, 1360, 1275, 811. Size exclusion chromatography: M_n = 21.6 kg/mol, $Đ$ = 1.72.

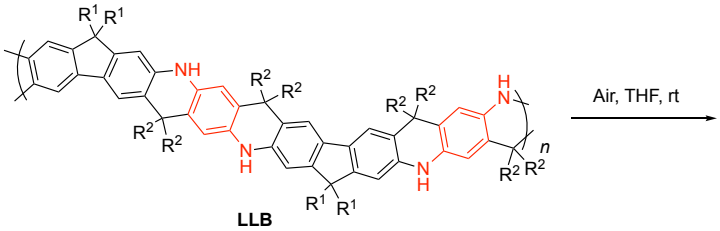

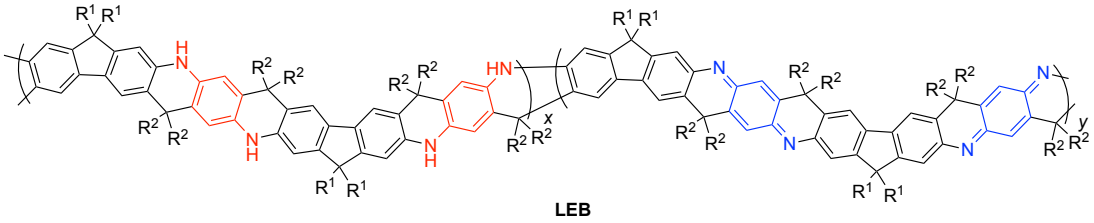

LEB: A **LLB** (0.10 g) solution in THF (10 mL) was gently stirred open in air for 12 h. The color turned from light yellow to dark green. After evaporating the solvent, the product **LEB** was collected as a black powder (0.1 g, quant.). ^{1}H NMR (500 MHz, THF-*d*8, 298 K) δ 7.17 – 6.14 (m, 16H), 1.72 (s, 6H), 1.42 – 0.96 (m, 40H), 0.86 (m, 10H). ^{13}C NMR (126 MHz, THF-*d*8, 298 K) δ 153.46, 151.83, 149.89, 144.54, 143.01, 142.82, 136.75, 135.85, 130.93, 130.61, 128.99, 128.56, 127.97, 127.00, 126.13, 125.17, 122.28, 120.12, 115.32, 107.99, 105.76, 58.22, 57.07, 54.83, 41.31, 32.66, 30.95, 30.43, 30.10, 23.37, 20.87, 14.27. FT-IR (ATR) (cm^{-1}): 3305, 2931, 2947, 1679, 1616, 1500, 1463, 1368, 1284, 810. Size exclusion chromatography: M_n =

24.3 kg/mol, $Đ$ = 1.95. Elemental analysis: C: 85.15%, H: 8.37%, N: 3.14%.

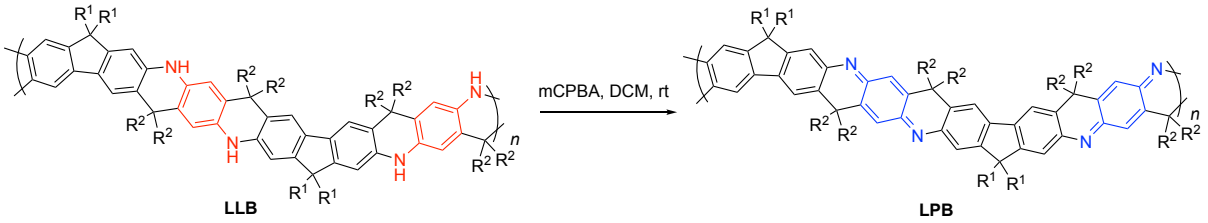

LPB: *meta*-chloroperoxylbenzoic acid (*m*CPBA) (2 equiv.) was added into a solution of **LLB** (0.10 g) in CH_2Cl_2 (10 mL). The mixture was stirred at room temperature for 12 h. After washing with water (10 ml × 3), the organic phase was dried over Mg_2SO_4. After removing the solvent by rotatory evaporator, **LPB** product was isolated as a blackish powder (0.10 g, quant.). ^{1}H NMR (500 MHz, THF-*d*8, 298 K) δ 7.12 – 6.59 (m, 12H), 2.30 (s, 24H), 1.17 (m, 80H), 0.86 (m, 20H). ^{13}C NMR (126 MHz, THF-d8, 298 K) δ 152.59, 143.09, 141.73, 141.05, 140.86, 139.31, 137.56, 135.89, 130.40, 129.41, 121.91, 119.89, 56.86, 56.27, 32.64, 30.41, 30.35, 30.06, 23.34, 20.86, 14.24. FT-IR (ATR) (cm^{-1}): 2921, 2852, 1689, 1604, 1510, 1468, 1363, 1289, 815. Size exclusion chromatography: M_n = 25.5 kg/mol, $Đ$ = 1.67.

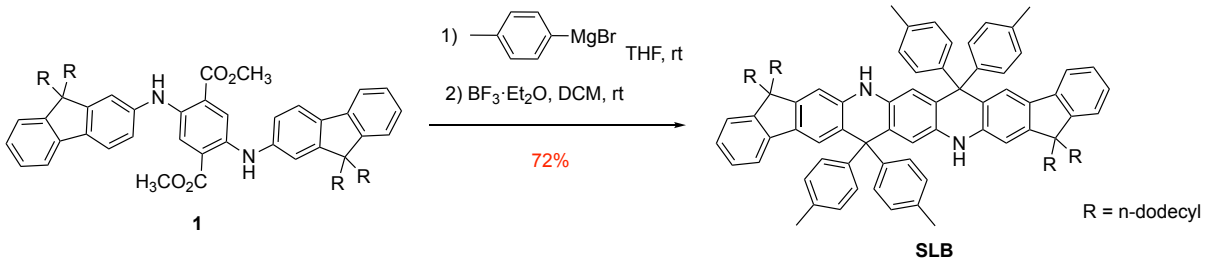

SLB: Compound **1** was synthesized according to a previously reported procedure.[2] *p*-Tolyl magnesium bromide (5 mL, 1.0 M in THF) was added into a dried flask under N_2 protection. Compound **1** (0.61 g, 0.50 mmol) was dissolved in THF (5 mL) and the solution was added into the mixture slowly. The mixture was stirred at reflux for overnight. After cooled to room temperature, the reaction was quenched with saturated NH_4Cl aqueous solution, and extracted with ethyl acetate for 3 times. The organic layers were combined and dried with $MgSO_4$. After removing solvent by rotatory evaporator, the crude product was dissolved in dry CH_2Cl_2 (10

mL). $BF_3 \cdot Et_2O$ (1 mL, 0.3 M) was added into the solution and the reaction was stirred at room temperature for 12 h in N_2 protection. The reaction was quenched with NaOH aqueous solution (1 M), and extracted with ethyl acetate. The combined organic layers were dried over $MgSO_4$ and purified with flash column chromatography (silica, hexane:CH_2Cl_2 v/v = 3:1). The pure product was collected as a while solid (0.53 g, 72%). ^{1}H NMR (500 MHz, *d*8-THF, 298 K) δ = 7.99 (s, 2H), 7.29 – 7.19 (m, 4H), 7.13 – 7.04 (m, 6H), 7.02 (abq, J = 8.2 Hz, 8H), 6.96 – 6.87 (abq, J = 8.2 Hz, 8H), 6.71 (s, 2H), 6.35 (s, 2H), 2.31 (s, 12H), 2.01 – 1.80 (m, 8H), 1.36 – 0.99 (m, 72H), 0.87 (t, J = 6.9 Hz, 12H), 0.72 (m, 4H). ^{13}C NMR (125 MHz, *d*8-THF, 298 K) δ = 150.86, 150.56, 145.31, 143.14, 142.54, 136.14, 135.22, 133.39, 131.40, 129.06, 128.32, 127.34, 126.96, 125.97, 123.29, 122.12, 119.23, 115.78, 108.33, 57.54, 55.39, 41.81, 33.02, 31.28, 30.76, 30.53, 30.45, 24.97, 23.72, 21.25, 14.64. HRMS (+ESI) calcd. [M+H+]: 1494.1402 found: 1494.1334.

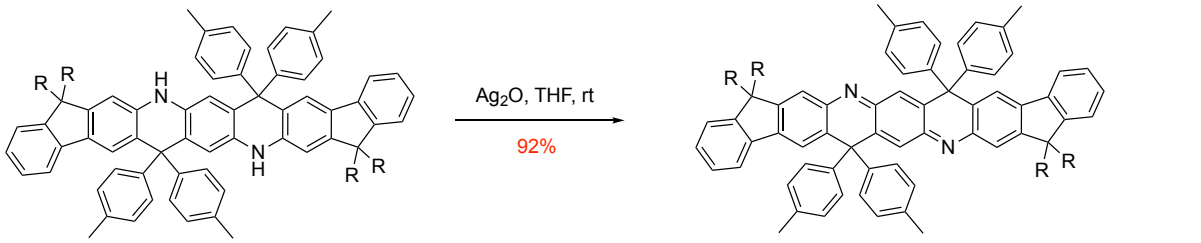

SLB **SPB** R = n-dodecyl

SPB: Ag_2O (0.10 g) was added into a solution of **SLB** (0.50 g, 0.33 mmol) in THF (20 mL). The mixture was stirred at room temperature for 12 h followed by filtration. The filtrate was collected and solvent was removed by rotatory evaporator. The crude product was further purified by flash column chromatography (silica, hexane/DCM v/v = 4:1). The product was collected as a dark red solid (0.46 g, 92%). ^{1}H NMR (500 MHz, *d*8-THF, 298 K) δ = 7.51 (s, 2H), 7.48 (d, J = 7.4 Hz, 2H), 7.36 (m, 4H), 7.23 (m, 4H), 7.10 (abq, J = 8.0 Hz, 8H), 7.01 (abq, J = 8.0 Hz, 8H), 6.68 (s, 2H), 2.34 (s, 12H), 2.04 (m, 8H), 1.36 – 1.04 (m, 72H), 0.87 (t, J = 6.7 Hz, 12H), 0.74 (m, 8H). ^{13}C NMR (125 MHz, *d*8-THF, 298 K) δ = 154.80, 152.52, 151.37, 146.08, 142.90, 142.87, 142.14, 141.64, 137.52, 136.79, 136.25, 130.98, 129.65,

128.50, 127.78, 125.72, 123.78, 122.09, 121.19, 58.68, 55.84, 41.30, 33.01, 31.18, 30.72, 30.44, 25.04, 23.73, 21.25, 14.67. HRMS (+ESI) calcd. [M+H+]: 1493.1279 found: 1493.1246.

3. Oxidation Titration

UV-Vis absorption spectra were recorded when a *m*CPBA solution was titrated from 0 to 1.0 equivalent into a solution of **LLB** in CH_2Cl_2 (concentration of repeating units = 8.3 mM). Clear isosbestic point indicated a clean transformation from **LLB** to **LPB.**

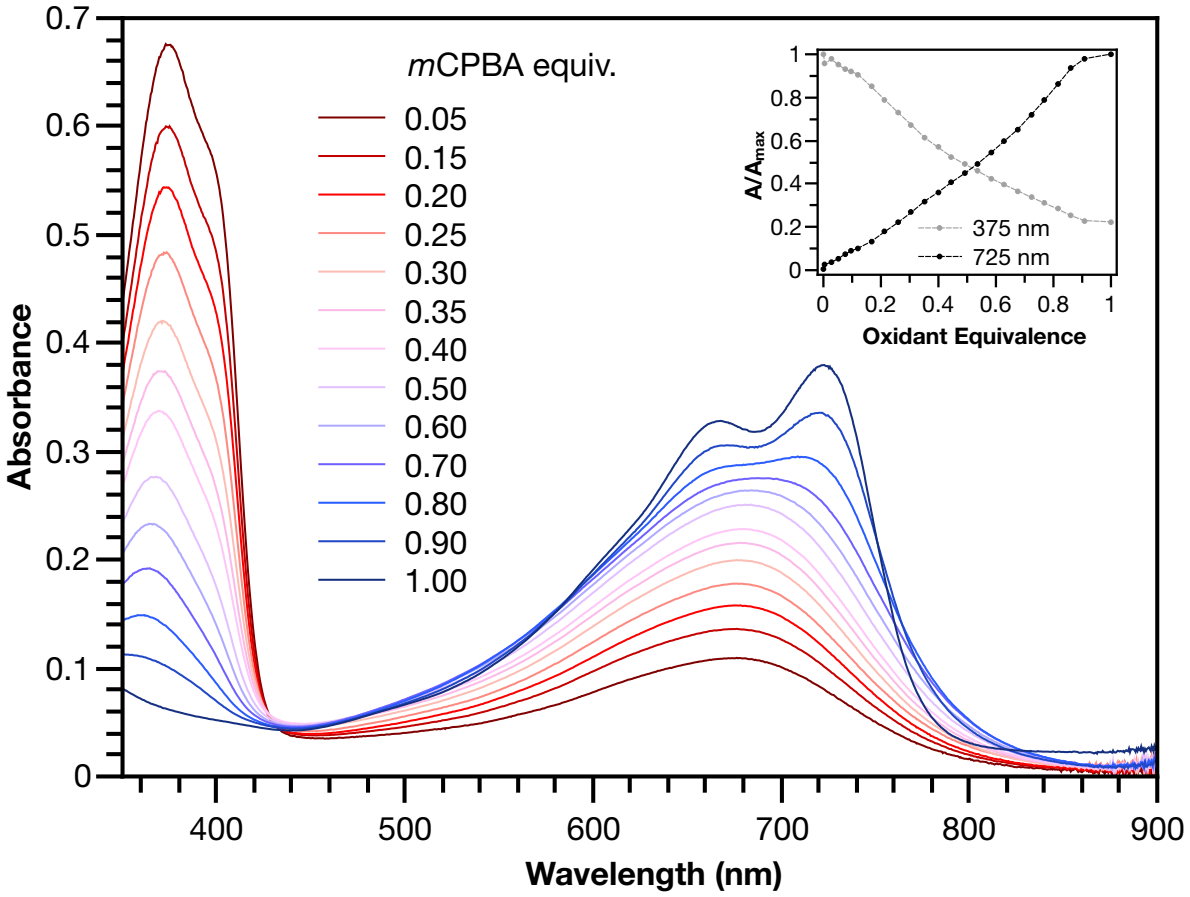

Figure S1. UV-vis spectra of a solution of **LLB** titrated with *m*CPBA in CH_2Cl_2.

4. FT-IR Spectroscopy

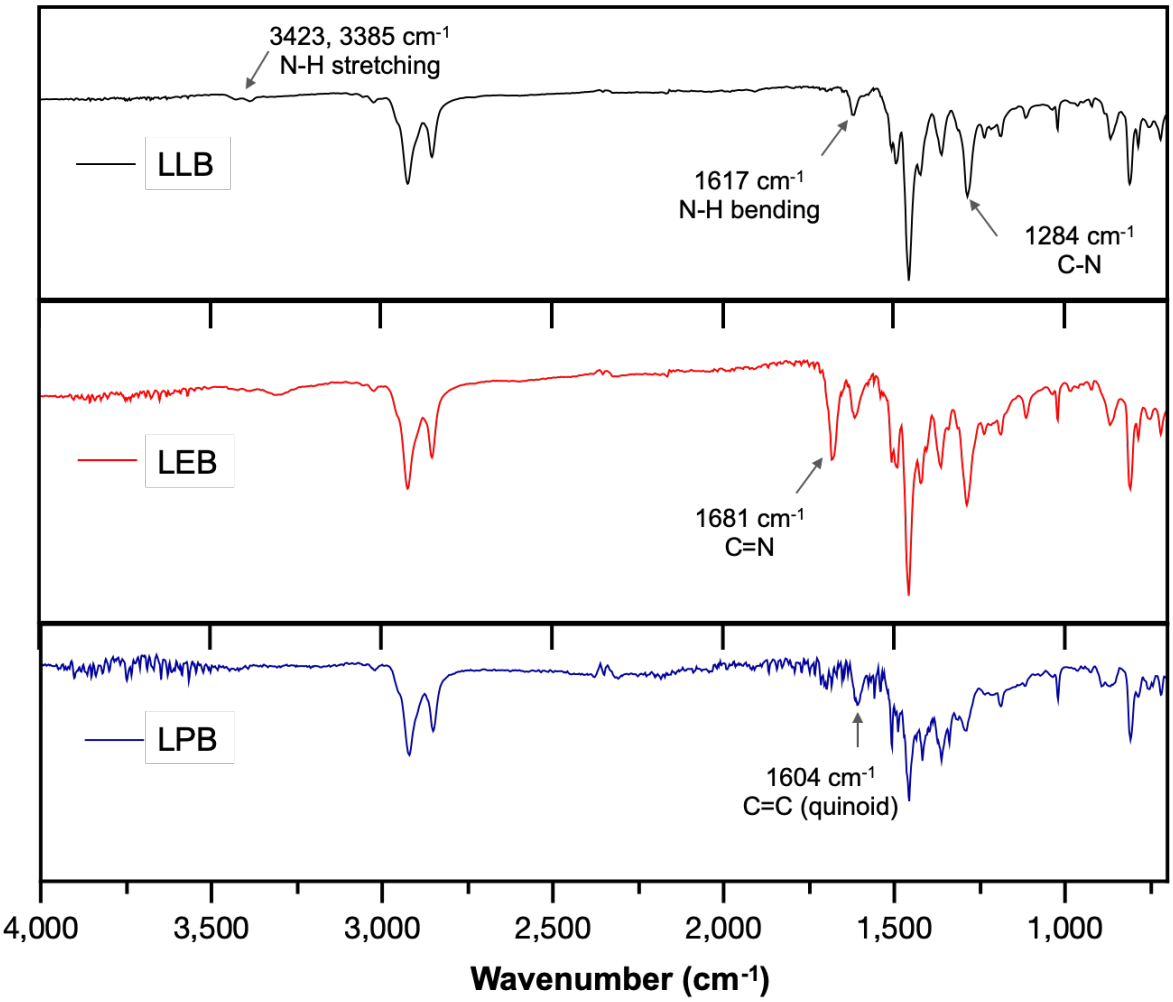

Figure S2. FT-IR spectra of **LLB**, **LEB**, and **LPB**.

5. Cyclic Voltammetry and Electrochemical Stability Measurement

Cyclic voltammetry (CV) was performed in a three-electrode system with Ag/AgCl as the reference electrode and a platinum wire as the counter electrode. Ferrocene/Ferrocene$^+$ (Fc/Fc^+) was used as the external reference. $TBAPF_6$ solution in THF (0.1 M), MSA in THF (0.15 M) and $LiClO_4$ solution in THF (1.2 M) were used as the electrolyte depending on the experimental setting. For solution-phase measurement, a 3 mm glass-carbon electrode was used as the working electrode. For thin-film measurement, a piece of ITO-coated glass with spin-coated polymer thin film was used as the working electrodes. **LPANI** sample was spin-coated on the

ITO-coated glass as a thin film from their chlorobenzene solutions (20 mg/mL, 2000 rpm for 120 s) and annealed at 110 ˚C for 10 min in glovebox. The scan rate was set as 100 mV/s.

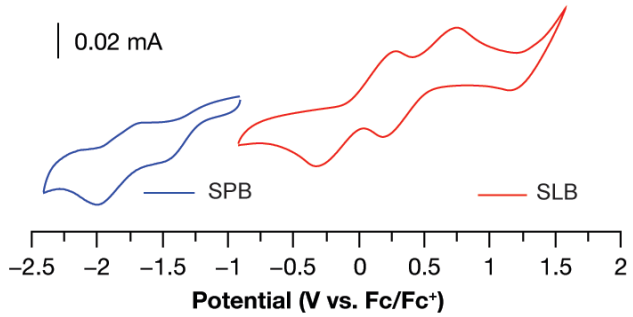

Figure S3. Cyclic voltammograms of **SLB** and **SPB** films in acetonitrile with $TBAPF_6$ (0.1 M).

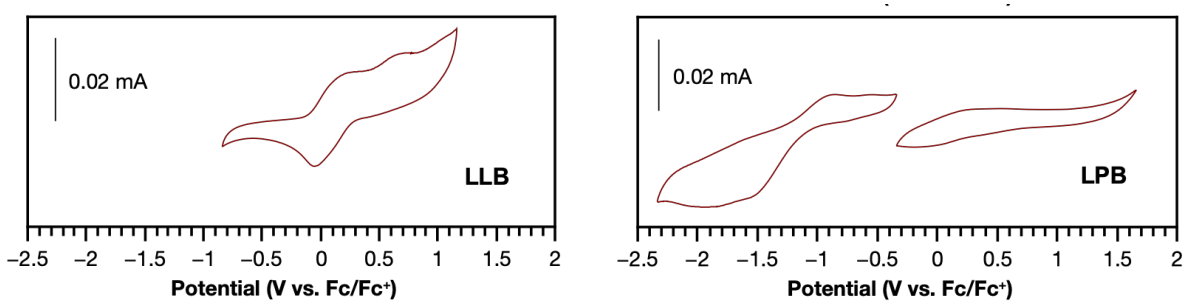

Figure S4. Cyclic voltammograms of **LLB** and **LPB** films in acetonitrile with $TBAPF_6$ (0.1 M).

The experiments on the electrochemical stability measurement were performed on **LPANI**-coated carbon fabric cloth working electrodes. The electrodes were held in the electrolyte containing 0.5 M of H_2SO_4 in acetonitrile, and controlled potentials of +1.0 V, +1.5 V, and +2.0 V were applied. After definite time periods, cyclic voltammograms were recorded, and the anodic peak current obtained was used to evaluate the degradation percentage. As a comparison, PANI was deposit on the carbon fabric cloth electrode with electropolymerization in aqueous solution with aniline (0.03 M) and H_2SO_4 (0.5 M) by scanning from -0.9 V to +0.5 V for 50 cycles. Then the electrode was washed with DI water and then acetonitrile. The degradation was measured using the same procedure.

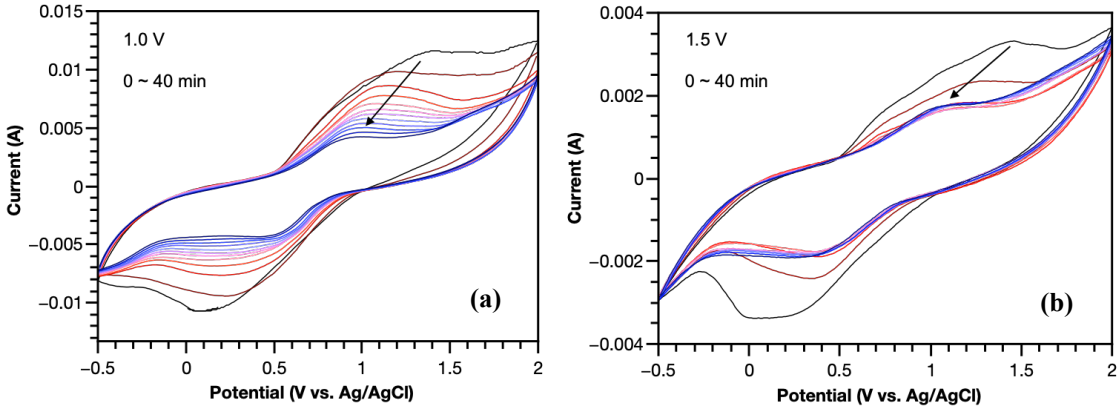

Figure S5. Cyclic voltammogram of PANI on carbon fabric cloth in a H_2SO_4 solution in acetonitrile (0.5 M). Oxidation potentials at (a) +1.0 V, and (b) +1.5 V were applied on the working electrode. The voltammograms were recorded after applying the potential for 0, 1, 2, 3, 5, 10, 15, 20, and 40 min, respectively.

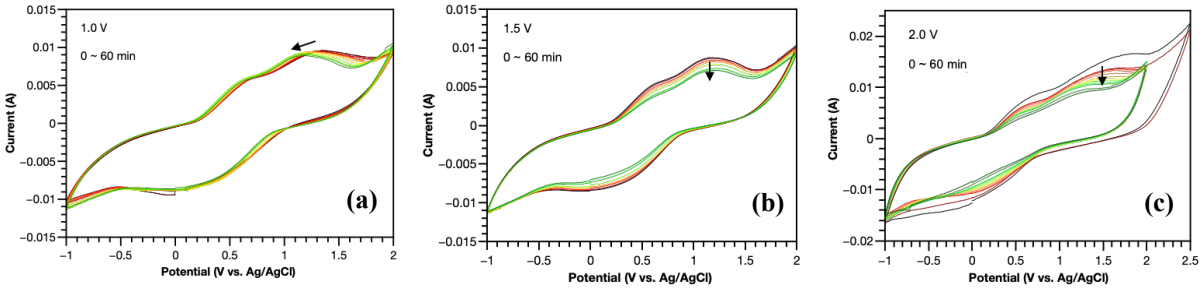

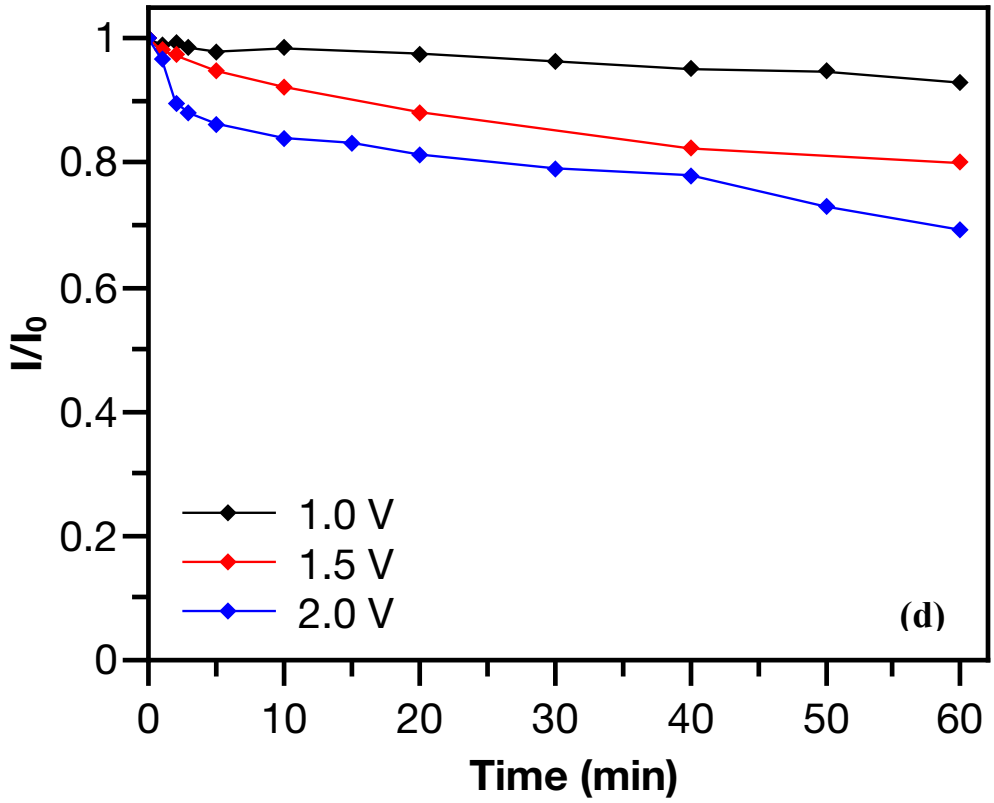

Figure S6. Cyclic voltammograms of **LPANI** on carbon fabric cloth in a H_2SO_4 solution in acetonitrile (0.5 M). Oxidation potentials at (a) +1.0 V, (b) +1.5 V, and (c) +2.0 V were applied on the working electrode. The voltammograms were recorded after applying the potential for 0, 1, 2, 3, 5, 10, 15, 20, 40, and 60 min, respectively. (d) Plots of current intensities in (a), (b), and (c) *vs* time.

6. Acid-doping and Stability Test

For stability measurement, a solution of **LPS** in THF with *ca.* 4 M methanesulfonic acid (MSA) was kept in ambient conditions. Visible-NIR absorption spectra were recorded from 0 min to 42 h (Figure S8a). The stability of **LPS** with excessive amount of *p*-toluenesulfonic acid (PTSA) in the thin film state was also measured after 1 week of storage in ambient condition (Figure S8b). In both cases, the major low bandgap absorption character was retained after the extensive acid treatment with only marginal changes observed on the spectra, indicating the

extraordinary stability of **LPS** against strong acid and hydrolysis.

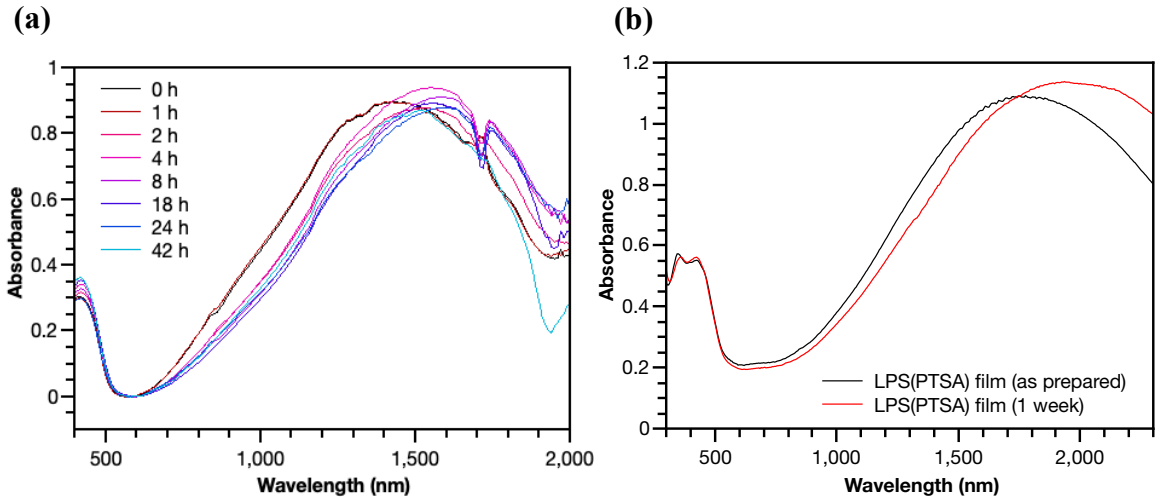

Figure S7. (a) Visible-NIR absorption spectra of **LPB** in THF with 4 M MSA over a period of 42 h; (b) Visible-NIR absorption spectra of as prepared acidified LPS thin film in the presence of PTSA, and the sample after 1 week stored under ambient condition.

7. Paramagnetism Characterization

Electron paramagnetic resonance (EPR) spectrometry was conducted on a Bruker ELEXSYS II E500 with microwave frequency of *ca.* 9.38 GHz at 288 K. A 4 mm ID sample tubes was used for solids samples. The spectra were acquired at 1 G modulation and 100 kHz modulation frequency. The *x*-axis represents the g factor, and the *y*-axis represents the intensity per mole of repeating unit. The *g* factors were calculated based on the following equation in which ν is the microwave frequency and *B* is the resonance magnetic field:

$$g = \frac{71.4484 \times \nu\ (GHz)}{B\ (mT)}$$

Magnetic measurements were conducted on a Quantum Design MPMS XL SQUID magnetometer from 2 to 300K. The magnetization measurements were performed at 2K over the magnetic field range of 250-70000 Oe. The diamagnetic contributions of the sample holders and the atoms were corrected with blank holders and the Pascal's constants.

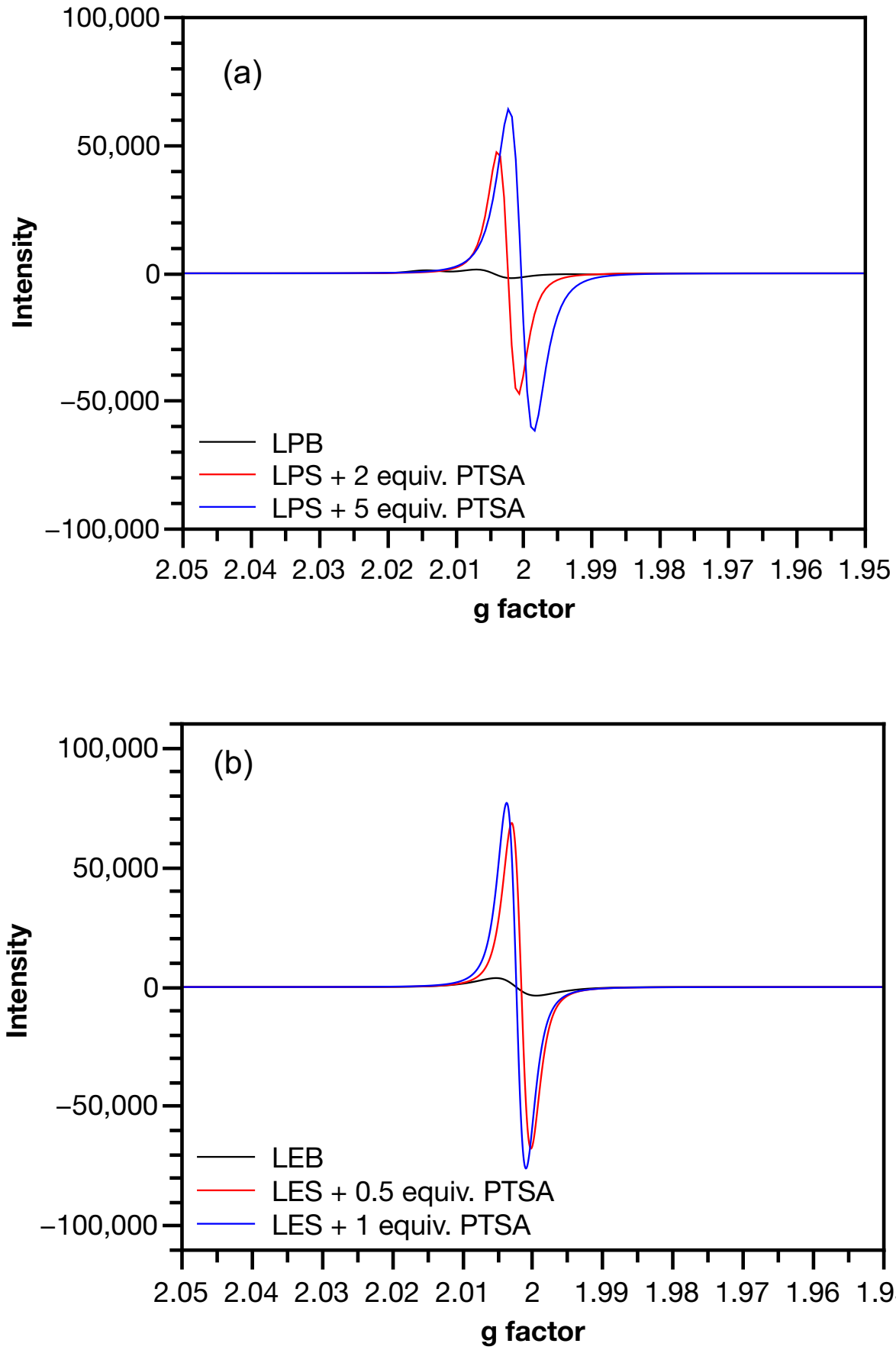

Figure S8. EPR spectra of (a) **LPS** and (b) **LES** solids doped with different molar equivalents

of PTSA. Each sample contained 1.0 mmol of cyclohexadiene-1,4-diimine units.

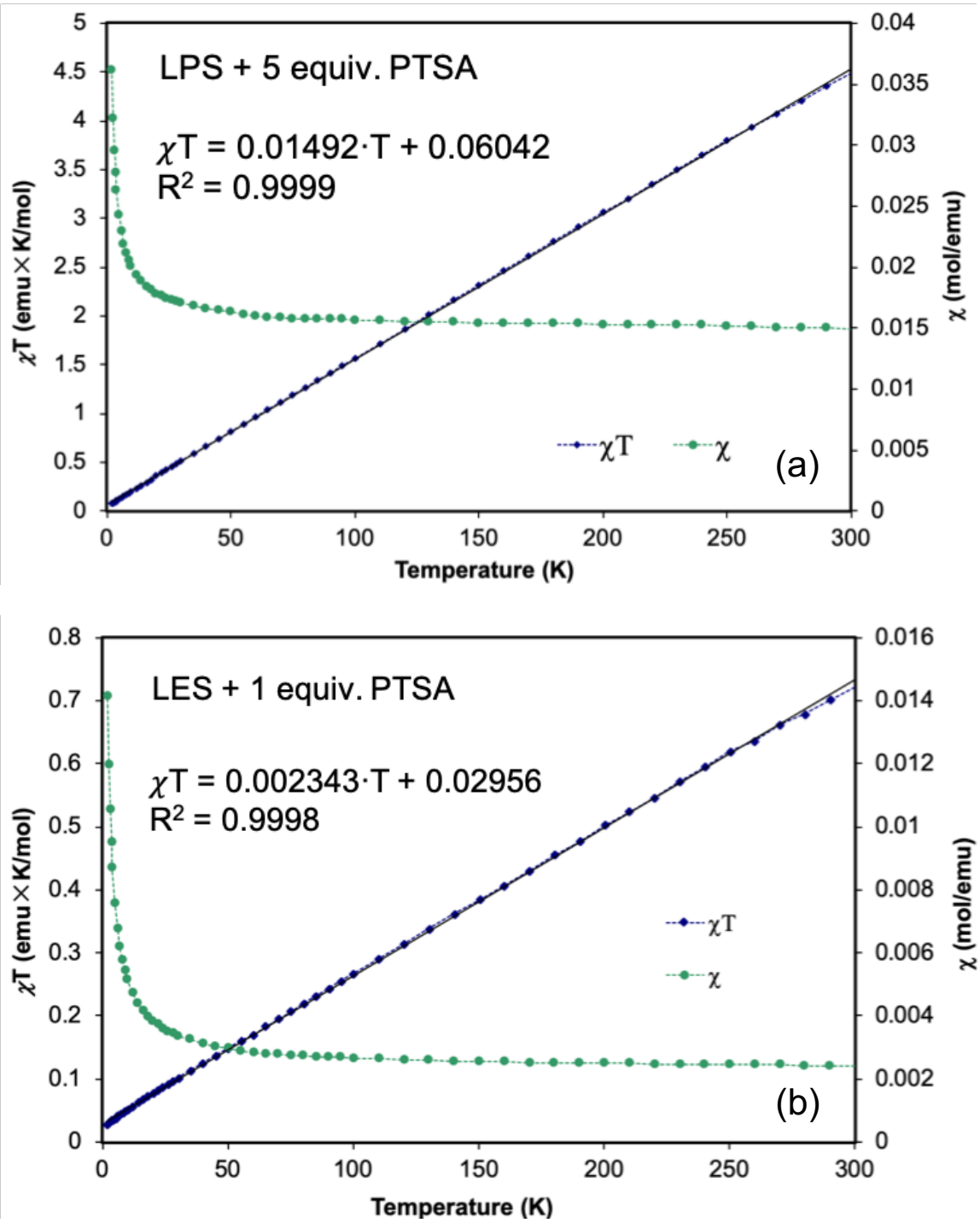

Figure S9. Varied-temperature paramagnetic susceptibility of (a) **LPS** and (b) **LES** solids doped with PTSA.

8. DC Conductivity

DC conductivity was measured by a four-point probe method under vacuum. Pellet samples of

LES and LPS were prepared by compressing the powder materials (~0.1 g) in a mold with inner diameter of 25 mm at pressure of 20 kPa in air. The electrical resistance was measured with a Keithley 2450 SourceMeter. The thickness of the pellet was measured using a profilometer as *ca*. 10^{-2} cm. The electrical conductivity was calculated based on the slope of the I-V plots.

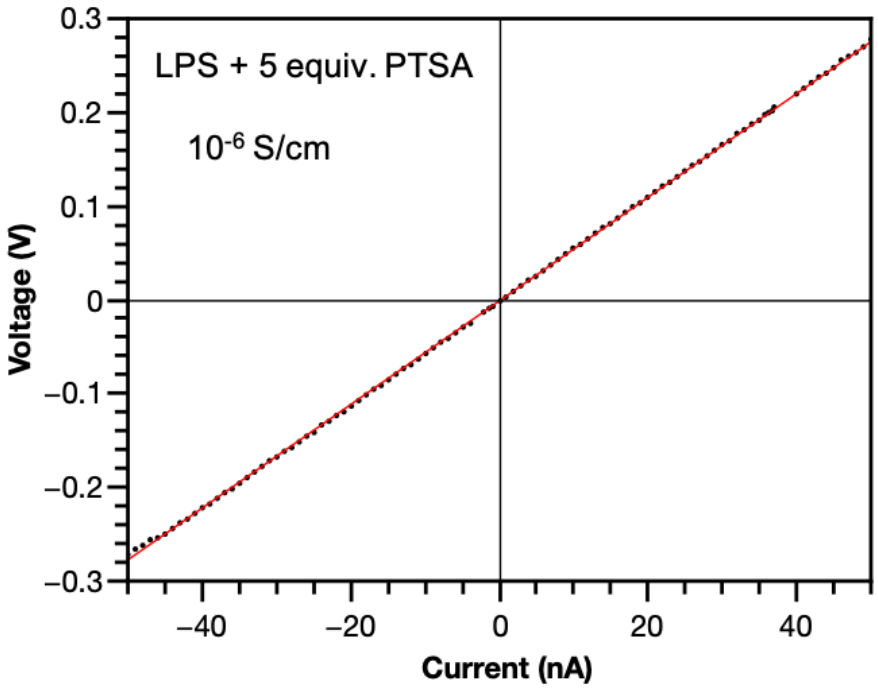

Figure S10. I-V plots of **LPS** pellets doped with PTSA using a four-probe method.

9. Electrochromic Device

Electrochromic devices were fabricated in a sandwich architecture. Gel electrolyte was prepared by mixing PMMA (MW: ~12000 g/mol, 2 g), propylene carbonate (5 mL), and dry $LiClO_4$ (0.8 g) in acetonitrile (1 mL) at 50 ˚C for 72 h. The uniform gel was degassed under vacuum to remove the solvent. Then the gel electrolyte was drop-cast on a 1-mm-thick ITO-coated glass substrate. On another ITO-coated glass, **LEB** thin film was spin-casted (500 rpm for 30 s, then 2000 rpm for 120 s) from its chlorobenzene solution (10 mg/mL) and the sample was annealed in a glovebox at 120 ˚C for 10 min. These two components were subsequently combined in a sandwich manner so that the gel layer and LEB layer were in contact with each

other. The resulting device was sealed with epoxy resin. The electrochromic response of the device was controlled with a potentiostat and recorded *in-situ* with a UV-vis-NIR absorption spectrometer. Voltage on working electrode was programed to switch between –2.0 V and +2.0 V, 30 s at each stage. The visible-NIR spectra were recorded accordingly. The switching process was recycled for 200 times to test the recycling performance of the device.

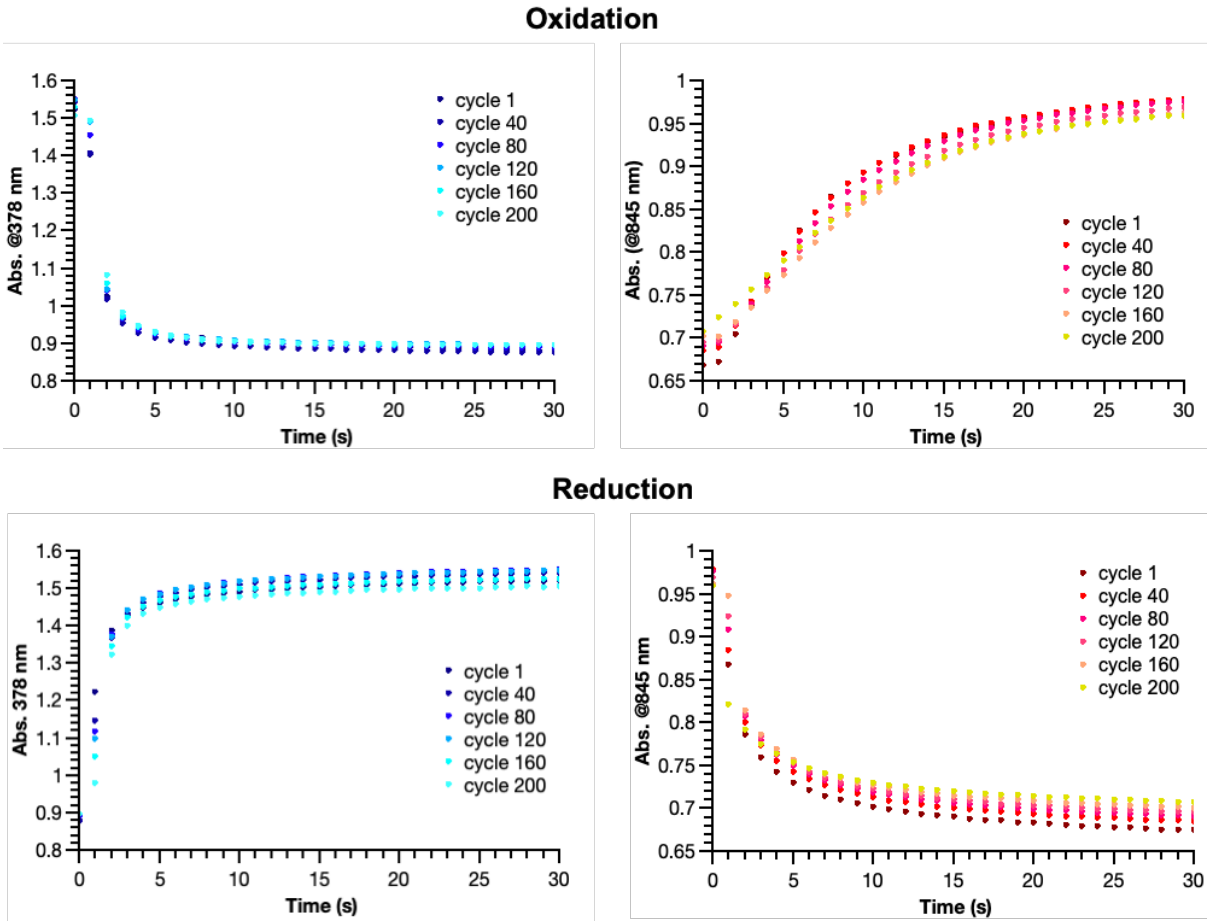

Figure S11. Time-dependent absorption of the electrochromic device at 378 nm and 845 nm at varied cycles.

The kinetics of oxidation and reduction processes were analyzed separately at both wavelengths. The time-dependent absorption plots of six cycles (Figure S11) were studied and they were all fit in first-order exponential equations shown in Table S1. The averaged fitting parameters of six cycles and corresponding standard deviation (STD) values were obtained.

Table S1. Kinetics fitting equation and parameters of plots in Figure S11

	378 nm	845 nm
Avg. $A_{oxi,0}$	0.893	0.991
STD	0.005	0.003
Avg. $A_{oxi,1}$	0.696	-0.323
STD	0.015	0.015
Avg. k_{oxi} (s^{-1})	0.556	0.101
STD	0.029	0.016
R^2	0.927~0.954	0.993~0.997
Avg. $A_{red,0}$	1.519	0.703
STD	0.015	0.010
Avg. $A_{red,1}$	-0.646	0.264
STD	0.013	0.020
Avg. k_{red} (s^{-1})	0.590	0.386
STD	0.077	0.042
R^2	0.955~0.989	0.942~0.980

10. Thermogravimetric Analysis

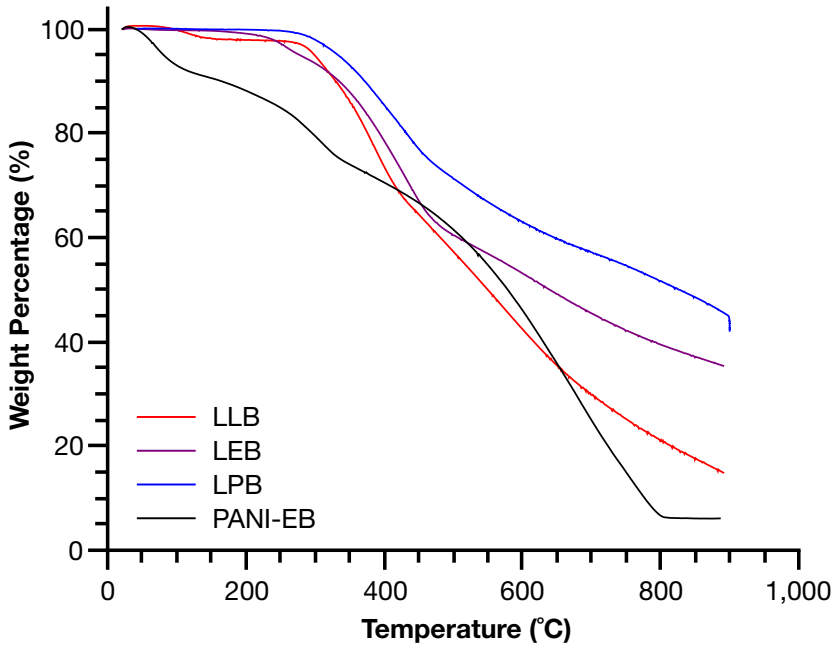

Figure S12. TGA plots of **LLB**, **LEB**, and **LPB**.

Thermogravimetric analysis (TGA) was undertaken with a TA Q500 thermogravimetric analyzer. Nitrogen flow was set as 60 mL/min. Temperature ramping was from 40 ˚C to 900

˚C with a rate of 10 ˚C/min.

Theoretical weight percentage values of backbone, alkyl chains, and tolyl groups are 29%, 34%, and 37%. The first stage in the range of 280 ~ 460 ˚C has 25%~36% weight loss for all three polymers. This stage could be attributed to the cleavage of alkyl chains on the fluorene moieties and agreed with reported examples. Above 500 ˚C, continuous weight loss was observed for all three polymers. For **LEB** and **LPB**, this stage could be attributed to continuous cleavage of Tolyl groups and the conversion of sp3 carbon into more thermodynamically favorable sp2 carbon. While for **LLB**, the backbone also underwent thermal degradation. Compared with the conventional polyaniline-emeraldine base, much higher thermal stability was observed in ladder polymers, especially when the temperature is below 300 ˚C.

11. NMR spectra

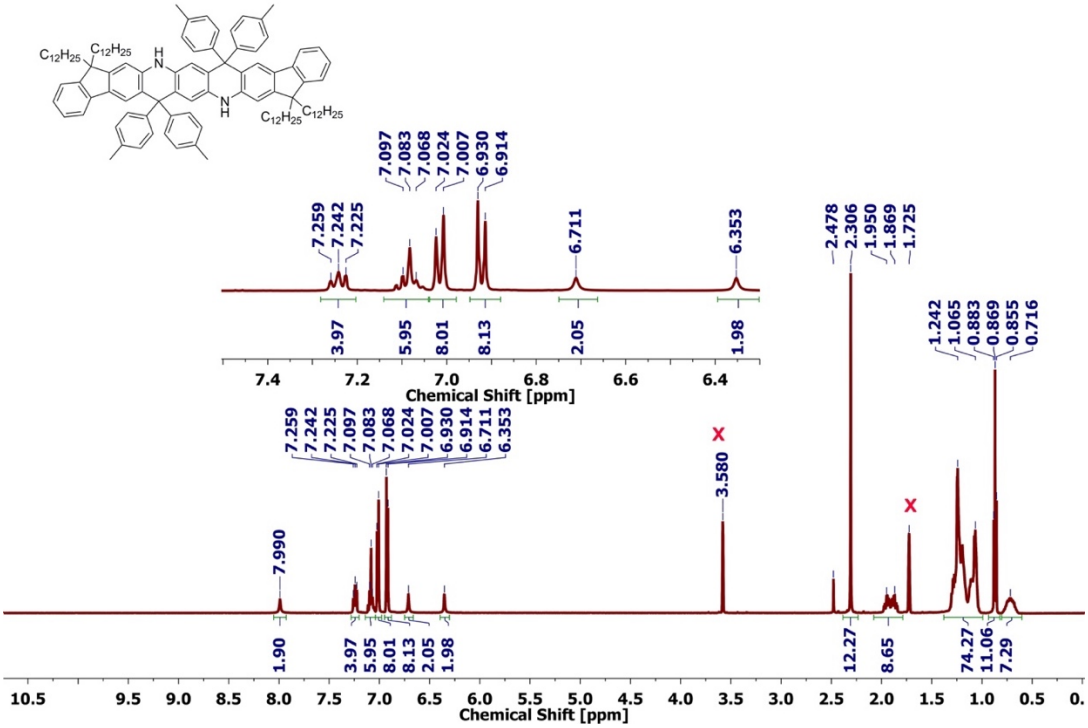

Figure S13. ^{1}H NMR spectrum of **SLB** in THF-*d*8 (500 MHz, rt).

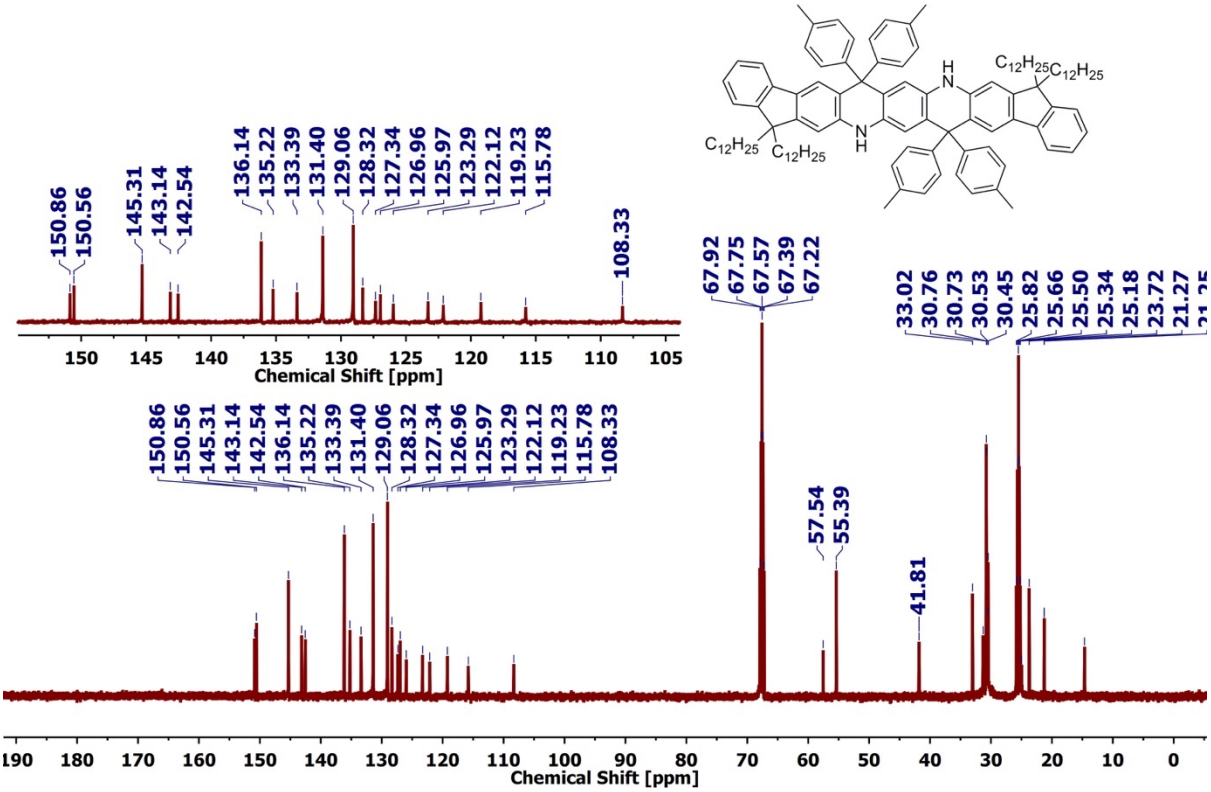

Figure S14. ^{13}C NMR spectrum of **SLB** in THF-*d*8 (126 MHz, rt).

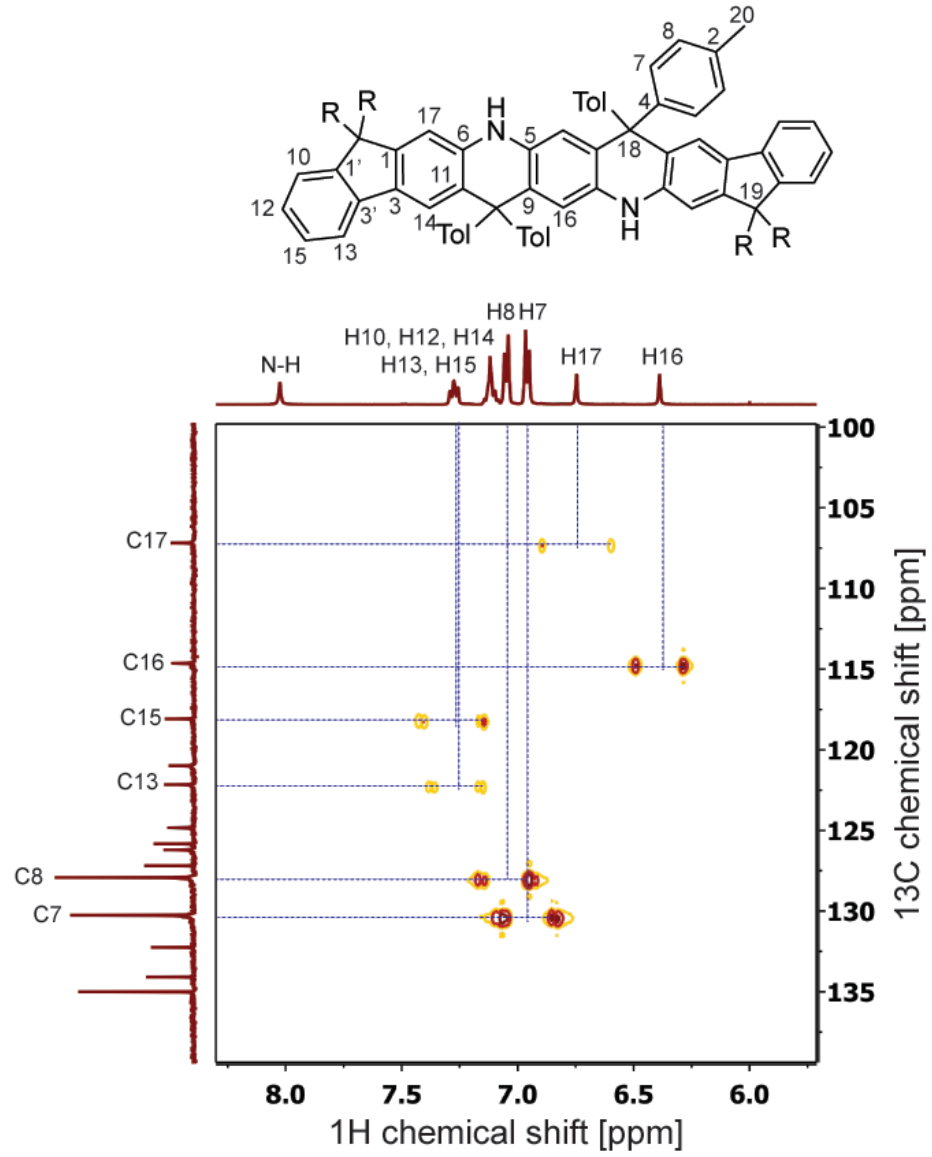

Figure S15. ^{1}H-^{13}C HSQC NMR spectrum of **SLB** in THF-*d*8 at RT.

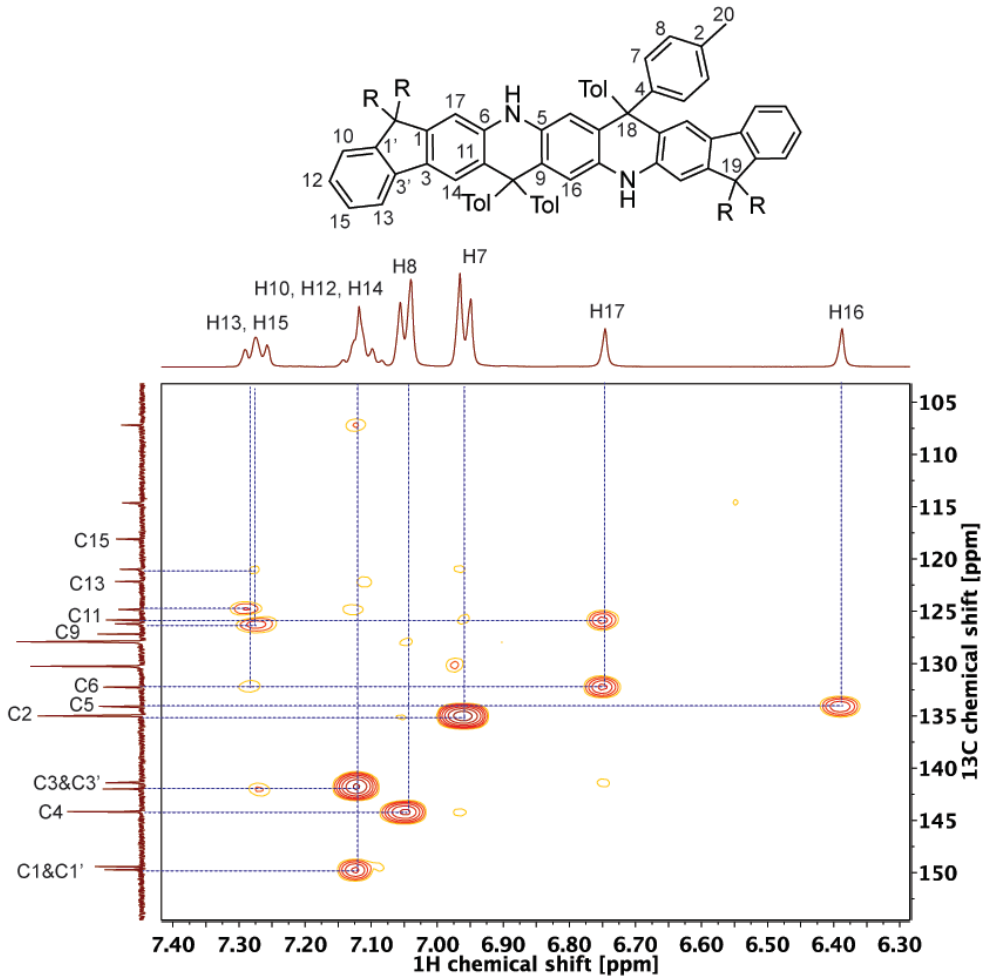

Figure S16. ^{1}H-^{13}C HMBC NMR spectrum of **SLB** in THF-*d*8 at RT.

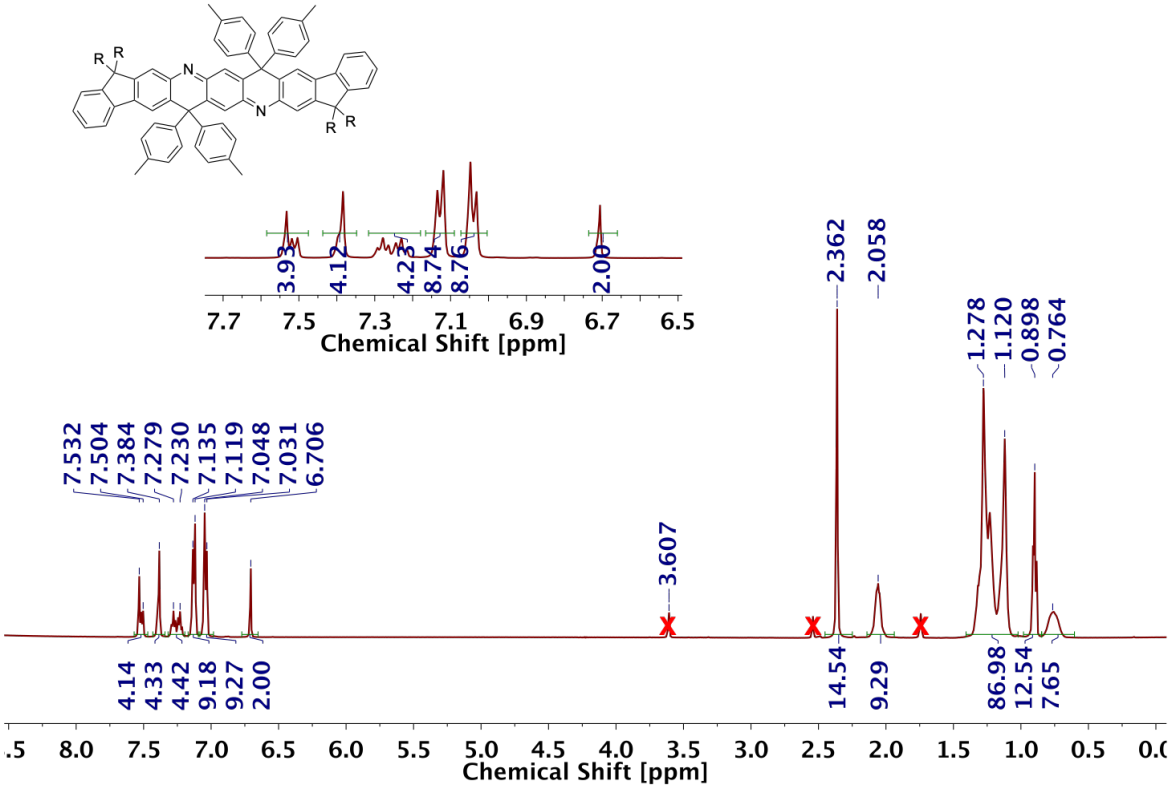

Figure S17. ^{1}H NMR spectrum of **SPB** in THF-*d*8 (500 MHz, RT).

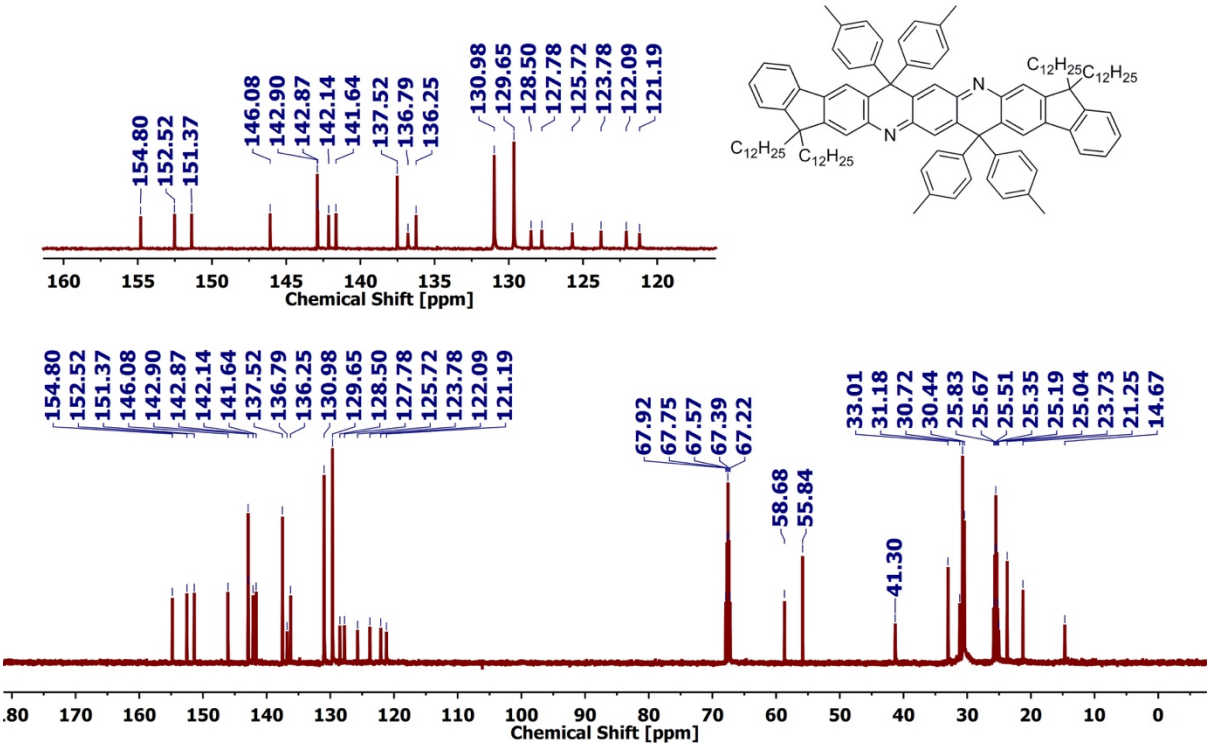

Figure S18. ^{13}C NMR spectrum of **SPB** in THF-*d*8 (126 MHz, RT).

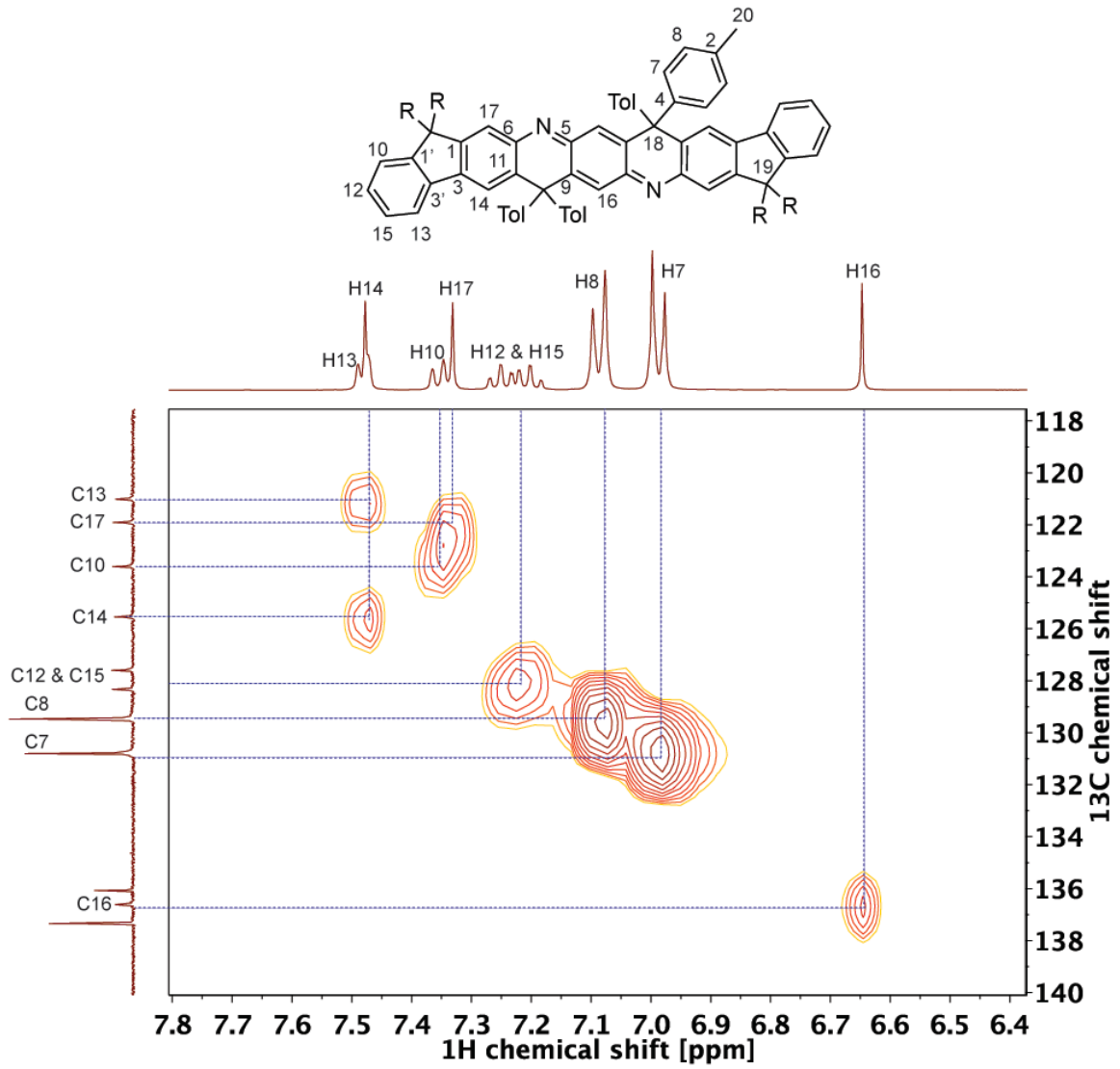

Figure S19. ^{1}H-^{13}C HSQC NMR spectrum of **SPB** in THF-*d*8 at RT.

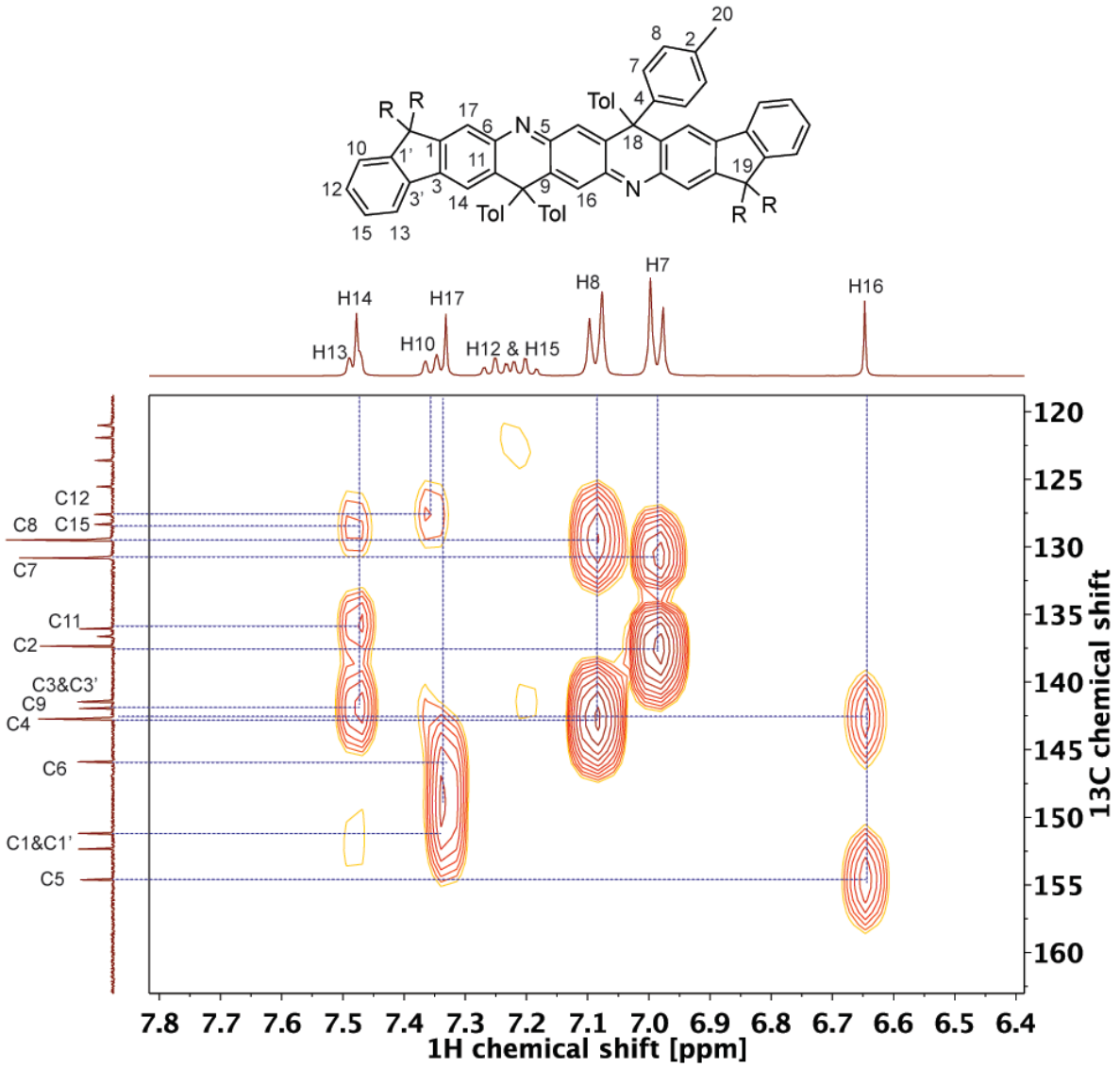

Figure S20. ^{1}H-^{13}C HMBC NMR spectrum of **SPB** in THF-*d*8 at RT.

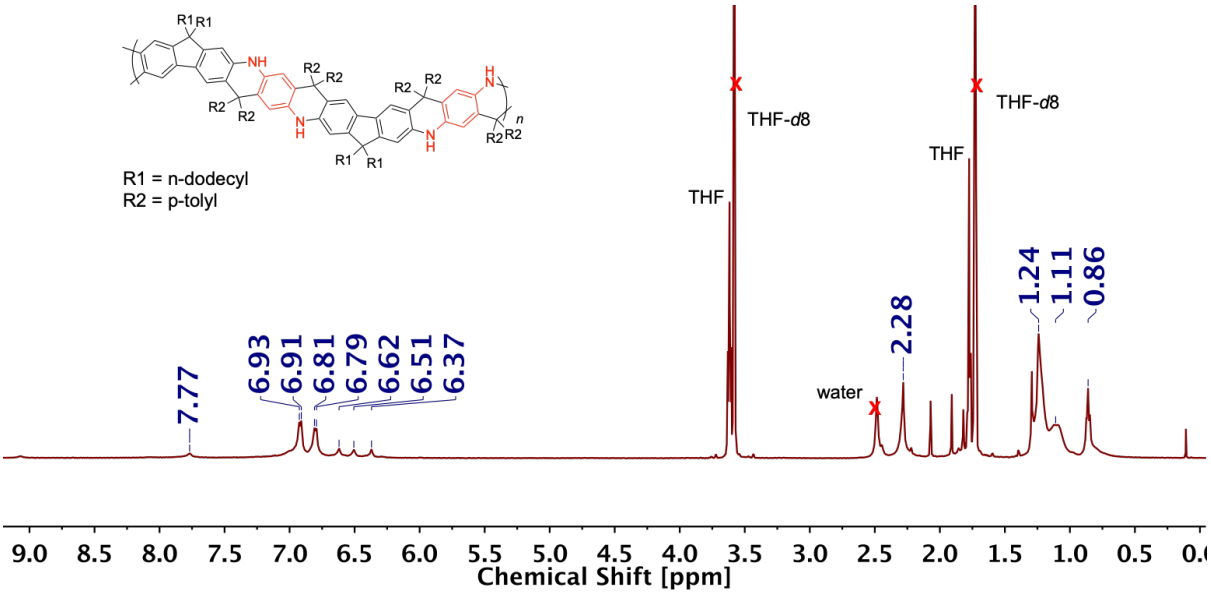

Figure S21. ^{1}H NMR spectrum of **LLB** in THF-*d*8 (500 MHz, RT).

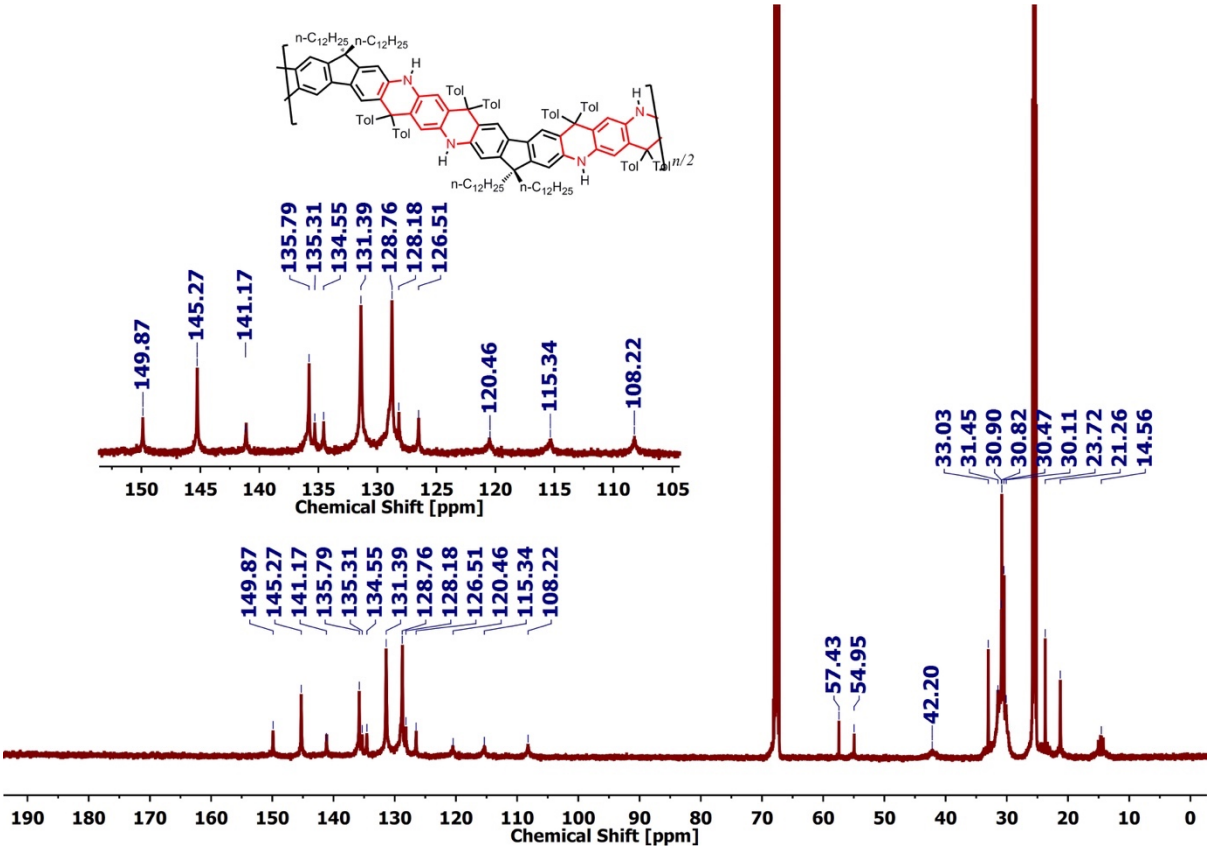

Figure S22. ^{13}C NMR spectrum of **LLB** in THF-*d*8 (126 MHz, RT).

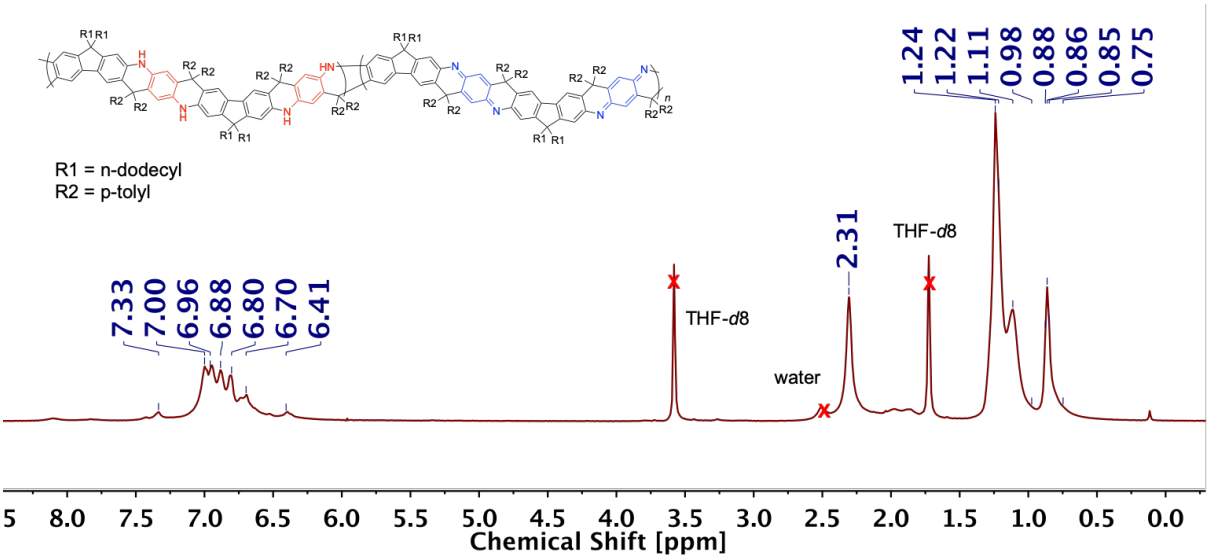

Figure S23. ^{1}H NMR spectrum of **LEB** in THF-*d*8 (500 MHz, RT).

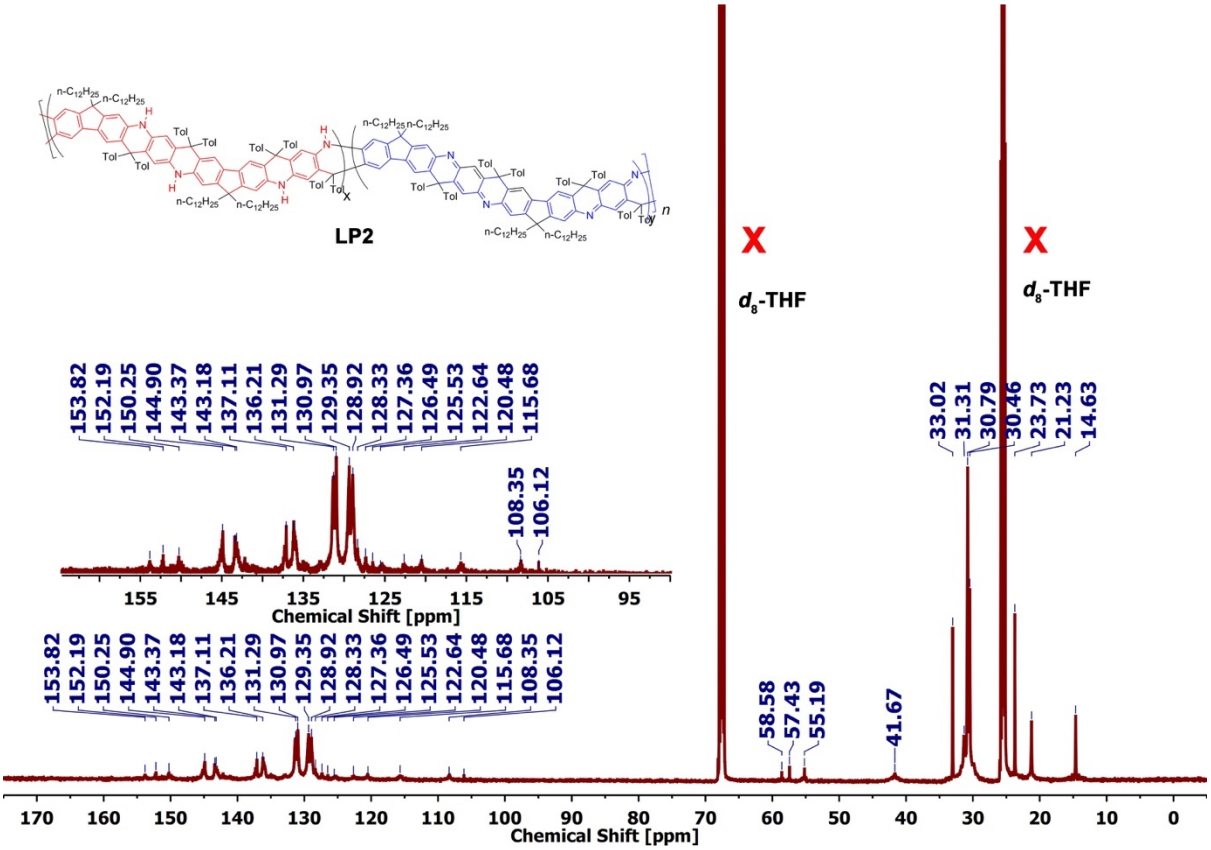

Figure S24. ^{13}C NMR spectrum of **LEB** in THF-*d*8 (126 MHz, RT).

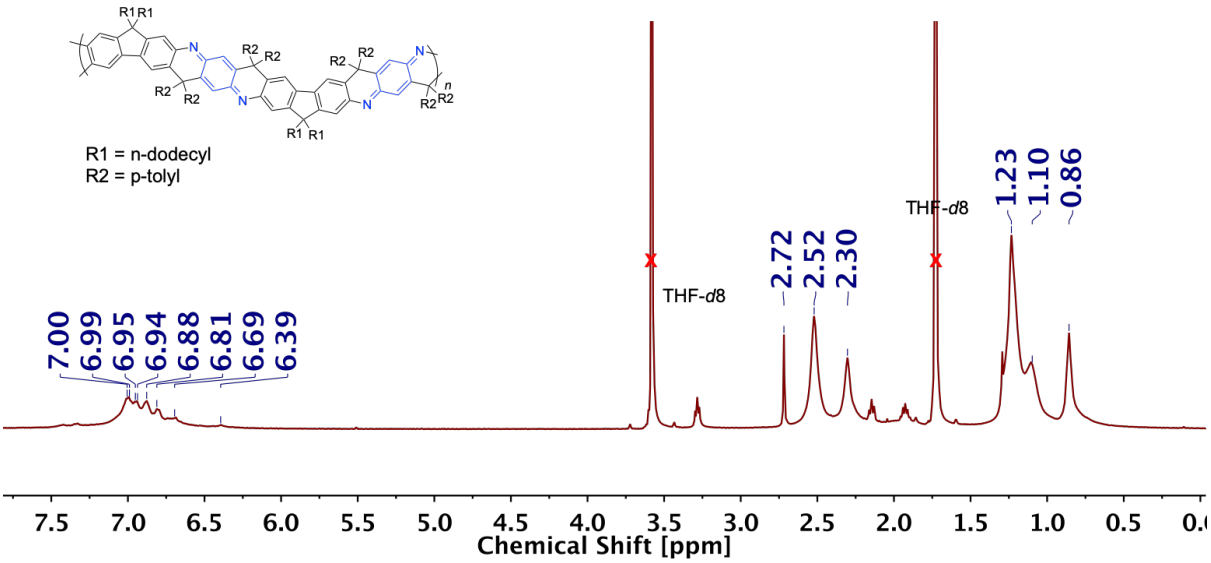

Figure S25. ^{1}H NMR spectrum of **LPB** in THF-*d*8 (500 MHz, RT).

References

[1] Y. Zou, X. Ji, J. Cai, T. Yuan, D. J. Stanton, Y.-H. Lin, M. Naraghi, L. Fang, *Chem* **2017**, *2*, 139-152.

[2] Y. Zou, T. Yuan, H. Yao, D. J. Frazier, D. J. Stanton, H.-J. Sue, L. Fang, *Org. Lett.* **2015**, *17*, 3146-3149.